

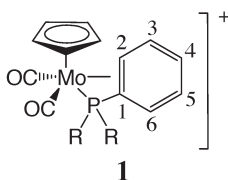
**REMOTE METAL–ARENE  $\pi$  BONDING IN ORGANOMETALLIC COMPLEXES: A DFT STUDY**Paulo J. COSTA<sup>a1</sup>, Maria José CALHORDA<sup>a2,\*</sup> and Paul S. PREGOSIN<sup>b</sup><sup>a</sup> Departamento de Química e Bioquímica, Faculdade de Ciências, Universidade de Lisboa, 1749-016 Lisboa, Portugal; e-mail: <sup>1</sup> pjcosta@fc.ul.pt, <sup>2</sup> mjc@fc.ul.pt<sup>b</sup> Laboratorium für Anorganische Chemie, ETHZ, Hönggerberg, 8093 Zürich, Switzerland; e-mail: pregosin@inorg.chem-ethz.chReceived March 5, 2007  
Accepted March 23, 2007*Dedicated to Dr Karel Mach on the occasion of his 70th birthday.*

The observation that the 14-electron cation  $[\text{Rh}(\text{PPh}_3)_3]^+$  is more electron-rich than expected, as a result of coordination of a C=C bond in one phenyl group, opened the way to a search for more examples of this behavior. We used DFT calculations and energy decomposition analysis to study this M– $\eta^2$ -arene interaction and to calculate its strength. For this purpose, we have chosen two formally unsaturated complexes, viz.  $[\text{Mo}(\eta^5\text{-C}_5\text{H}_5)(\text{CO})_2(\text{PPh}_3)]^+$  (**1**) and  $[\text{Ru}(\eta^5\text{-C}_5\text{H}_5)(\text{binap})]^+$  (**2**). In the former complex, the  $\text{PPh}_3$  ligand can be easily moved away from the metal, destroying the Mo– $\eta^2$ -arene interaction, while in **2** this is achieved by a distortion of the Binap ligand. The experimental parameters, namely the distortion of the aryl-containing ligand, have been well reproduced by the calculated coordination geometry; the M– $\eta^2$ -arene interaction was estimated as 13.4 kcal mol<sup>-1</sup> for Mo and 21.4 kcal mol<sup>-1</sup> for Ru. The energy decomposition analysis revealed the formation of a covalent bond between the metal and the C=C bond, which made the global process favorable, regardless the energy required to reorganize the geometry of the ligand in the new environment.

**Keywords:** Rhodium; Ruthenium; Molybdenum; Arene complexes; Energy decomposition analysis (EDA); DFT calculations; Binap; Phosphine ligands; Half-sandwich complexes.

Phosphanes are among the most common ligands in organometallic chemistry, offering a wide range of electronic and steric features. Moreover, they stabilize a large number of compounds designed for applications in homogeneous catalysis. Triphenylphosphane, a crystalline solid, is often the first choice for a monodentate phosphane. However, in 1984 it was revealed that the phenyl groups were not always only spectator substituents. They are capable of binding to the Rh(I) metal center through a C=C bond, hereby stabilizing the coordinatively unsaturated metal center, by donation of additional two electrons<sup>1</sup>. Indeed, the 14-electron cation  $[\text{Rh}(\text{PPh}_3)_3]^+$  has

achieved a 16-electron count as a consequence of a coordinated C=C bond, with Rh–C distances of 2.236 and 2.502 Å. In recent years, a number of other examples was reported. The cation  $[\text{Mo}(\eta^5\text{-C}_5\text{H}_5)(\text{CO})_2(\text{PPh}_3)]^+$  (**1**) is formally an 18-electron complex, since one of the phenyl rings binds to the metal using a C=C bond, as in the Rh example, with Mo–C distances of 2.566 and 2.649 Å to C1 and C2, respectively (Chart 1)<sup>2</sup>. These distances are relatively long, but apparently still within the bonding range. Reactions of **1** with MeI or H<sub>2</sub>O lead to fast disappearance of the bond. In the unambiguous  $\eta^2\text{-C}_6\text{H}_6$  complex  $[\text{Ru}(\eta^5\text{-C}_5\text{Me}_5)(\eta^2\text{-C}_6\text{H}_6)(\text{NO})]$ , the Ru–C distances to the C=C bond are 2.195 and 2.221 Å, i.e., apparently shorter than those in **1**, but close to one of the Rh–C bonds in  $[\text{Rh}(\text{PPh}_3)_3]^+$ <sup>3</sup>.



1

CHART 1

This type of weak coordination is not peculiar only to PPh<sub>3</sub>. Similar situations have also been observed in the more interesting chiral bidentate phosphanes, MeO-biphep and binap (MeO-biphep = 6,6'-dimethoxy-2,2'-bis(di-R-phosphanyl)-1,1'-biphenyl; binap = 2,2'-bis(diphenylphosphanyl)-1,1'-binaphthyl). Although their complexes are very useful as chiral auxiliaries in enantioselective catalysis, the specific  $\eta^2$ -arene interaction was initially not detected in reports describing the syntheses and characterization of these and other phosphane complexes of Ru(II)<sup>4</sup>. Later on, more detailed studies<sup>5–7</sup> showed that one C=C bond in one of the phenyl rings was bound to ruthenium, as sketched for the cationic Ru diphosphane complexes in Chart 2, with Ru–C distances of 2.257 and 2.280 Å in  $[\text{Ru}(\eta^5\text{-C}_5\text{H}_5)\text{-(binap)}]^+$  (**2**)<sup>5</sup>, and 2.383 and 2.311 Å in  $[\text{Ru}(\eta^5\text{-C}_5\text{H}_5)(\text{MeO-biphep})]^+$  (**3**)<sup>6</sup>. These species are often fluxional, with the Ru atom jumping between the two rings. There has been continued interest in this type of weak bond, as documented by a recent series of crystal structure studies of transition metal complexes on this topic<sup>8</sup>. Further,  $\eta^2$ -arene coordination was also observed in the crystal structure of lanthanoid derivatives, contributing to a partial compensation of the electron deficiency at the metal centers<sup>9</sup>. Several review articles have also appeared<sup>10</sup>. Increasingly, intermediates or transition states in catalytic reactions featuring such interactions have been proposed. For example, a chiral ligand was assigned an assisting role in the

enantioselective hydrovinylation of styrene catalyzed by Ni(II) complexes<sup>11</sup>. Similar interactions have been proposed in other systems<sup>12</sup>, including luminescent gold complexes<sup>13</sup>.

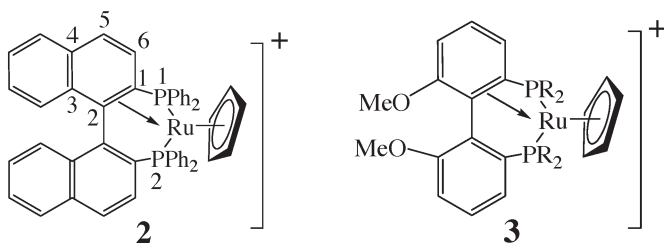


CHART 2

As might be expected from Charts 1 and 2, the ligands in 1–3 must distort so that one C=C bond in the aromatic rings approaches the metal center and binds. A similar distortion of phenyl rings has been described in other complexes, namely  $[\text{Rh}(\text{H})(\text{Cl})(\text{SiCl}_3)(\text{PPh}_3)_2]$ <sup>14</sup>, where the metal center is involved in an agostic interaction<sup>15</sup> with one C–H bond of the phenyl, allowing Rh(III) to achieve the 18-electron count. In order to understand the nature of the  $\eta^2$ -arene bonding and to estimate its energy, we performed DFT calculations on two model complexes,  $[\text{Mo}(\eta^5\text{-C}_5\text{H}_5)(\text{CO})_2(\text{PPh}_3)]^+$  (1; Chart 1) and  $[\text{Ru}(\eta^5\text{-C}_5\text{H}_5)(\text{binap})]^+$  (2; Chart 2).

### COMPUTATIONAL DETAILS

Density functional theory (DFT) calculations<sup>16</sup> were carried out with the Amsterdam density functional (ADF-2004) program<sup>17</sup>. The local spin density exchange correlation potential was used with the local density approximation of the correlation energy (Vosko, Wilk and Nusair<sup>18</sup>). Gradient-corrected geometry optimizations<sup>19</sup> were performed using the generalized gradient approximation (Perdew–Wang nonlocal exchange and correlation corrections – PW91)<sup>20</sup>.

A triple- $\zeta$  Slater-type orbital basis set augmented by two polarization functions was used for Mo, Ru, P, O, C, and H. A frozen-core approximation was used to treat the core electrons: (1s) for C and O, (1s, 2p) for P, ([1-3]s, [2-3]p, 3d) for Mo and Ru. Relativistic effects were accounted with the ZORA approximation<sup>21</sup>.

Mayer indices<sup>22</sup>, calculated with the ADF implementation, were used as bond strength indicators. Wiberg indices<sup>23</sup> were obtained from a natural population analysis<sup>24</sup> (NPA) using the GENNBO executable of the Natural

Bond Orbital 5.0 program<sup>25</sup> (NBO) included in the ADF distribution. As this calculation requires all electron basis sets in ADF, the same types of basis sets described above were used without the frozen-core approximation for the NPA calculations.

The interactions between the metals and the C–C bonds were analyzed with the energy decomposition analysis (EDA) method developed by Ziegler and Rauk<sup>26</sup>. In this method, the bond dissociation energy ( $\Delta E = -D_e$ ) between two fragments is taken as the sum of two terms contributions,  $\Delta E = \Delta E_{\text{prep}} + \Delta E_{\text{int}}$ .  $\Delta E_{\text{prep}}$  is the energy required to reorganize the fragments from their equilibrium geometry to the geometry of the complex.  $\Delta E_{\text{int}}$  is the interaction energy between the two fragments in the complex and can be divided into three components  $\Delta E_{\text{elec}} + \Delta E_{\text{Pauli}} + \Delta E_{\text{orb}}$ . The  $\Delta E_{\text{elec}}$  term corresponds to the electrostatic interaction energy between the fragments,  $\Delta E_{\text{Pauli}}$  is the repulsive interaction between the fragments as a result of the fact that two electrons with the same spin are unable to occupy the same region in space,  $\Delta E_{\text{orb}}$  is associated with the orbital interaction energy (covalent bond formation).

## RESULTS AND DISCUSSION

### Structures

We have chosen two complexes to address the nature of the  $\eta^2$ -arene interaction and to estimate its energy.  $[\text{Mo}(\eta^5\text{-C}_5\text{H}_5)(\text{CO})_2(\text{PPh}_3)]^+$  (**1**) exhibits a coordination environment around the metal that can easily be switched from the 18-electron (Chart 1) to the 16-electron count, by moving the phosphane P atom away from the molybdenum, thereby breaking the bond between Mo and the C=C bond. The distortion is not so easily achieved in the larger complex  $[\text{Ru}(\eta^5\text{-C}_5\text{H}_5)(\text{binap})]^+$  (**2**). However, binap is an extremely important chiral ligand in active catalytic systems, and it is important to inspect what happens in the selected binap complex (Chart 2).

The structure of complex **1** was experimentally determined using synchrotron radiation<sup>2</sup>. DFT<sup>16</sup> calculations were performed using the ADF program<sup>17</sup> (PW91 functional<sup>20</sup>) on complex **1** and its model, where two phenyl groups were replaced by hydrogen atoms (**1m**). The experimental Mo–P–C1 angle in **1** is 73.0°, far away from the normal angles around coordinated phosphorus. This distortion permits the C=C bond to approach Mo and bind. We also allowed this angle to open, increasing the Mo–C1 and Mo–C2 distances, so that the phosphane became a two-electron donor (model **1m'**).

There is also an experimental crystal structure available for  $[\text{Ru}(\eta^5\text{-C}_5\text{H}_5)\text{-(binap)}]^+$  (**2**)<sup>5</sup>, with short Ru–C1 and Ru–C2 distances (2.257 and 2.280 Å, respectively; see Chart 2). One of the P–C=C moieties acts as a four-electron donor while the other one, on the opposite side of the molecule (not numbered in Chart 2), is a two-electron donor. The complex is formally an 18-electron species. Owing to the fairly large size of the molecule, we have only optimized the structure of model **2m**, similar to the X-ray structure of **2**, but with R = H. An analogue of the 16-electron complex has been built by moving the C=C bond of Binap away from ruthenium, eliminating the Ru–C1/C2 interaction (model **2m'**). The geometry was optimized at the DFT (PW1) level of theory.

The optimized geometries of  $[\text{Mo}(\eta^5\text{-C}_5\text{H}_5)(\text{CO})_2(\text{PPh}_3)]^+$  (**1**), and the two models **1m** and **1m'** are shown in Fig. 1, and of the models **2m** and **2m'** of  $[\text{Ru}(\eta^5\text{-C}_5\text{H}_5)(\text{binap})]^+$  (**2**) in Fig. 2. The relevant structural parameters are reported in Table I for **1** and in Table II for **2**.

The agreement between the calculated values for **1** and the experimental results is excellent and the interaction between the molybdenum center and the C1=C2 bond is very well reproduced (2.566 and 2.647 Å in the X-ray structure, 2.594 and 2.647 Å in the optimized one). One of the phenyl groups in the phosphane is highly distorted, as evidenced by the experimental Mo–P–C1 angle of 73.0°. The remaining two Mo–P–C angles are 117.7 and 131.3°. The calculated values are also very close, viz. 73.4, 117.5 and 130.2°, respectively.

The substitution of two phenyl groups by two hydrogen atoms (**1m**) leads to shortening of the Mo–P distance in comparison with **1**, while the Mo–C1 and Mo–C2 bond lengths slightly increase. The remaining paramete-

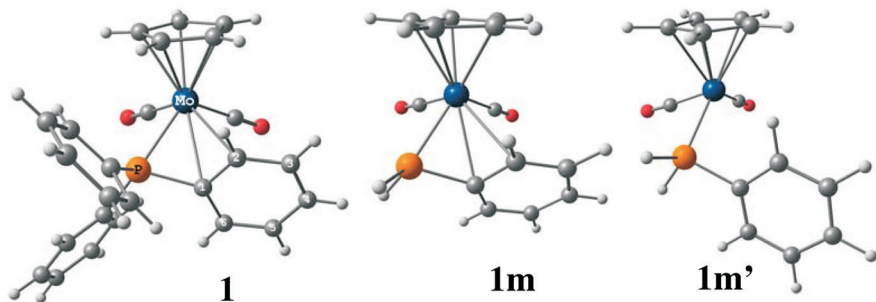


FIG. 1  
Optimized geometries (DFT) of complex  $[\text{Mo}(\eta^5\text{-C}_5\text{H}_5)(\text{CO})_2(\text{PPh}_3)]^+$  (**1**), and the two models **1m** and **1m'**

TABLE I

Experimental (X-ray) and calculated (DFT) distances (in Å) and angles (in °) of complex  $[\text{Mo}(\eta^5\text{-C}_5\text{H}_5)(\text{CO})_2(\text{PPh}_3)]^+$  (**1**), its two models **1m** and **1m'**, and relative energies (in kcal mol<sup>-1</sup>)

Bond	<b>1</b> (X-ray)	<b>1</b>	<b>1m</b>	<b>1m'</b>
Mo–P	2.430	2.445	2.409	2.444
Mo–C1	2.566	2.594	2.617	3.333
Mo–C2	2.647	2.647	2.678	3.526
C1–C2	1.418	1.422	1.424	1.410
C2–C3	1.422	1.411	1.412	1.392
C3–C4	1.362	1.381	1.381	1.393
C4–C5	1.404	1.410	1.410	1.398
C5–C6	1.368	1.380	1.381	1.391
C6–C1	1.444	1.418	1.417	1.403
Mo–P–C1	73.0	73.4	75.4	102.0
$\Delta E$	–	–	0	13.4

TABLE II

Experimental (X-ray) distances (in Å) and angles (in °) of complex  $[\text{Ru}(\eta^5\text{-C}_5\text{H}_5)(\text{binap})]^+$  (**2**), the calculated (DFT) data for its two models **2m** and **2m'**, and relative energies (in kcal mol<sup>-1</sup>)

Bond	<b>2</b> (X-ray)	<b>2m</b>	<b>2m'</b>
Ru–P1	2.332	2.291	2.332
Ru–P2	2.327	2.268	2.306
Ru–C1	2.257	2.276	3.310
Ru–C2	2.280	2.332	3.879
C1–C2	1.465	1.446	1.392
C2–C3	1.488	1.476	1.433
C3–C4	1.425	1.424	1.435
C4–C5	1.467	1.435	1.415
C5–C6	1.333	1.358	1.372
C6–C1	1.466	1.441	1.418
Ru–P1–C1	64.4	66.5	105.0
$\Delta E$	–	0	21.4

ters calculated for **1m** are still acceptable, as the slightly larger deviations are all within the acceptable range. The calculated Mo–P–H angles in **1m** are 126.4 and 129.4°. These values are very different from the Mo–P–C angle in **1** (~118°). The model **1m'** (see also Table I) is formally a 16-electron species and its energy is higher by 13.4 kcal mol<sup>-1</sup> than that for **1m**. The calculated Mo–C1 and Mo–C2 distances are long (3.333 and 3.526 Å, respectively) and, therefore, consistent with a “normal” phosphane bonding mode. The Mo–P distance (2.444 Å) is slightly larger than the value calculated for **1m** (2.409 Å) and, obviously, the Mo–P–C1 angle (102.0°) is much wider than the same angle in **1m**.

The calculated geometry of model **2m** agrees very well with the experimental structure **2**, despite the absence of the phenyl groups attached to phosphorus. The structures in Fig. 2 show clearly that C1 and C2 are bound to Ru in **2m**, but noncoordinated in **2m'**. This change is reflected in the much longer Ru–C1 and Ru–C2 bonds in **2m'**, accompanied by the strengthening of the C1=C2 bond due to absent donation to Ru(II) and back-donation from ruthenium to the double bond. The calculated Ru–C distances are in excellent agreement with those for **2**, and are also very close to the Ru–C bond lengths in related complexes of RuCp with MeO-biphep (2.311 and 2.383 Å). Further, the angle between the two vectors C1–C4 in each phenyl ring of the binaphthyl moieties drops by ca. 15° upon coordination, a trend observed in other literature structures<sup>6</sup>.

For this cation, the energy of the model **2m'** is 21.4 kcal mol<sup>-1</sup> higher than that of **2m**. Obviously, in both systems, the ligand (PPh<sub>3</sub> or binap) must distort to a smaller or larger extent to achieve the modified geometry.

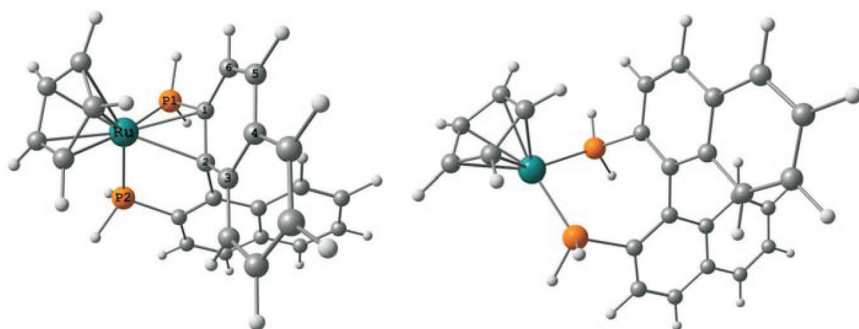


FIG. 2  
Optimized geometries (DFT) of the two models **2m** and **2m'** of the complex [Ru( $\eta^5$ -C<sub>5</sub>H<sub>5</sub>)-(binap)]<sup>+</sup> (**2**)

Therefore, in a first approach, the interaction energy will depend on the interaction itself and on the energy needed to change the geometry of the ligand from one situation to the other.

Before addressing this point, we will discuss the strength of the bonds by means of the Mayer bond orders, also called Mayer indices (MI), which are often more reliable as bond strength indicators than the distances. Apart from providing another perspective with respect to how changes in bond strength accompany geometric changes, they also provide a more reliable interpretation. The calculated MI for the two studied systems are given in Table III.

All the molybdenum models display very similar MI values for the Mo-P bonds (~0.8). The Mayer indices for the Mo-C1 and Mo-C2 bonds in **1** are 0.227 and 0.254. These values can be considered to reflect strong bond, since the corresponding Mo-C<sub>sp</sub> bond indices are ~0.3 (not shown). In model **1m**, the Mo-C1 MI decreases but the Mo-C2 MI increases. The changes, however, are small and **1m** can be considered a good model of complex **1** on both geometrical and electronic grounds. Curiously, in both calculations, the Mo-C2 distance is longer than Mo-C1, but the Mayer index is larger. In **1m'**, the calculated MIs for the Mo-C1 and Mo-C2 bonds are small, indicating the disappearance of the Mo...C=C interaction. The concomitant slight increase in the C1-C2 bond order reflects the absence of olefin bonding in this model, while in **1** and **1m**, the back-donation from the Mo dπ orbitals to the π\* orbital of the C1-C2 bond, and donation from the corresponding π orbital to Mo, should contribute to the slight weakening and bond elongation.

TABLE III

Mayer indices for relevant bonds in complex [Mo(η<sup>5</sup>-C<sub>5</sub>H<sub>5</sub>)(CO)<sub>2</sub>(PPh<sub>3</sub>)<sup>+</sup> (**1**), its two models **1m** and **1m'**, as well as the two models **2m** and **2m'** of complex [Ru(η<sup>5</sup>-C<sub>5</sub>H<sub>5</sub>)(binap)]<sup>+</sup> (**2**)

Bond	<b>1</b>	<b>1m</b>	<b>1m'</b>	<b>2m</b>	<b>2m'</b>
M-P1	0.846	0.822	0.862	0.883	0.919
M-P2	-	-	-	1.016	1.031
M-C1	0.227	0.188	0.088	0.288	0.025
M-C2	0.254	0.260	0.061	0.497	0.014
C1-C2	1.122	1.123	1.236	1.102	1.403



We also calculated the Wiberg indices (WI) for models **1m** and **1m'**, for comparison (not shown). These indices have been more widely used and usually provide reliable answers to problems, but require all electron basis sets in the ADF implementation, increasing the computational effort. Despite small differences, the trends are the same as found for the calculated MI. For instance, the calculated WI values for the Mo–P bond were  $\sim 0.6$  in **1m** and **1m'** while the MI values were  $\sim 0.8$  also for both models.

The trends are also similar in the  $[\text{Ru}(\eta^5\text{-C}_5\text{H}_5)(\text{binap})]^+$  (**2**) models **2m** and **2m'**. The Ru–P MIs change only very slightly from one model to another, showing that the Ru–P bonds are not influenced by the coordination of the C=C bond. The drop in the bond strength for the Ru–C bonds upon going from **2m** to **2m'** is much more significant than in the Mo system, probably due to the large size of Binap that allows the carbon atoms to move further away. For the same reason, the MI for C=C increases from 1.123 in **1m** to 1.236 Å in **1m'**, and from 1.102 in **2m** to 1.403 Å in **2m'**. Despite the electronic differences between  $d^4$  Mo(II) and  $d^6$  Ru(II), which contribute to different bond weakening upon coordination, the C=C bond in Binap becomes much stronger when moving away. It should be noted, however, that there is a large difference in the charges on the two bonded carbons, the more remote C2 atom having a  $-0.025$  charge and C1 being more negative ( $-0.063$ ).

### Energy Decomposition Analysis

Having introduced suitable models, as analyzed above, we performed an EDA in order to obtain an estimation of the  $\eta^2$ -arene interaction. For this purpose, we decomposed the two models **1m** and **1m'** of  $[\text{Mo}(\eta^5\text{-C}_5\text{H}_5)(\text{CO})_2(\text{PPh}_3)]^+$  (**1**), and the two models **2m** and **2m'** of complex  $[\text{Ru}(\eta^5\text{-C}_5\text{H}_5)(\text{binap})]^+$  (**2**) into fragments. The fragments are  $\{\text{Mo}(\eta^5\text{-C}_5\text{H}_5)(\text{CO})_2\}^+$  and  $\text{PPh}_2$  for models of **1**, and  $\{\text{Ru}(\eta^5\text{-C}_5\text{H}_5)\}^+$  and Binap for models of **2**. The results of the energy decomposition are given in Table IV.

The  $\eta^2$ -arene interaction ( $D_e$ ), given in the last row of Table IV was calculated as 8.58 and 13.74 kcal mol $^{-1}$  for the Mo and Ru complexes, respectively. These values arise from the balance between the reorganization of the fragments that exhibit different geometries in each of the two models, and the electronic interaction (the formation of the M–C bonds), and it is more relevant to analyze the differences. The metal fragments are only slightly modified when the C=C no longer coordinates, so that the values of  $\Delta E_{\text{prep}}(\text{M})$  are very small. The ligands must adapt more extensively,

in particular binap. Indeed,  $E_{\text{prep}}(\text{L})$  is 19.45 kcal mol<sup>-1</sup> for binap and only 4.21 kcal mol<sup>-1</sup> for PPhH<sub>2</sub>. Altogether, there is a large term accounting for the reorganization of binap in the Ru complex.

With respect to  $\Delta E_{\text{elec}}$ ,  $\Delta E_{\text{Pauli}}$ , and  $\Delta E_{\text{orb}}$ , the differences between  $\Delta E_{\text{orb}}$  dominate when going from **1m** to **1m'** (or **2m** to **2m'**), determining the outcome of the final term  $\Delta E_{\text{int}}$ , even if the other differences are not negligible, as happens in the Ru system.

TABLE IV

Energy decomposition for the interaction between L and M in models of [Mo( $\eta^5\text{-C}_5\text{H}_5$ )(CO)<sub>2</sub>(PPh<sub>3</sub>)]<sup>+</sup> (**1**) and [Ru( $\eta^5\text{-C}_5\text{H}_5$ )(binap)]<sup>+</sup> (**2**) (energy values in kcal mol<sup>-1</sup>)

Energy	<b>1m</b>	<b>1m'</b>	$\Delta$ ( <b>1m</b> - <b>1m'</b> )	<b>2m</b>	<b>2m'</b>	$\Delta$ ( <b>2m</b> - <b>2m'</b> )
$E_{\text{prep}}(\text{L})$	+7.38	+3.17	+4.21	+23.66	+8.30	+19.45
$E_{\text{prep}}(\text{M})$	+2.31	+2.11	+0.20	+8.96	+5.91	+3.05
$\Delta E_{\text{prep}}$	<b>+9.69</b>	<b>+5.28</b>	<b>+4.41</b>	<b>+32.62</b>	<b>+14.21</b>	<b>+28.21</b>
$\Delta E_{\text{elec}}$	-81.24	-87.33	+6.09	-217.38	-184.58	-32.80
$\Delta E_{\text{Pauli}}$	+112.45	+102.44	+10.01	+286.37	+217.46	+68.91
$\Delta E_{\text{orb}}$	-107.71	-78.62	-29.09	-215.29	-147.03	-68.26
$\Delta E_{\text{int}}$	<b>-76.50</b>	<b>-63.51</b>	<b>-12.99</b>	<b>-146.30</b>	<b>-114.15</b>	<b>-32.15</b>
$\Delta E = -D_e$	<b>-66.81</b>	<b>-58.23</b>	<b>-8.58</b>	<b>-113.68</b>	<b>-99.94</b>	<b>-13.74</b>

L = PPhH<sub>2</sub>, M = {Mo( $\eta^5\text{-C}_5\text{H}_5$ )(CO)<sub>2</sub>}<sup>+</sup> (**1m**, **1m'**) or L = binap, M = {Ru( $\eta^5\text{-C}_5\text{H}_5$ )}<sup>+</sup> (**2m**, **2m'**)

The emerging pattern is that the orbital interaction drops to 29.09 kcal mol<sup>-1</sup> (Mo) and 68.26 kcal mol<sup>-1</sup> (Ru) when the bond to C=C is lost. There is indeed a significant covalent interaction, and it is strong enough to cover the reorganization energy of the fragments.

The previous analysis allows us to conclude that in the formally 16-electron complexes analyzed it is energetically favorable to distort the ligand, so that one C=C bond of a phenyl ring may approach the metal and engage in a M- $\eta^2$ -arene bond, and the metal achieves an 18-electron count.

### Conclusions

The coordination between metal centers and ligands containing aryl rings was examined in detail for two complexes, [Mo( $\eta^5\text{-C}_5\text{H}_5$ )(CO)<sub>2</sub>(PPh<sub>3</sub>)]<sup>+</sup> (**1**)

and  $[\text{Ru}(\eta^5\text{-C}_5\text{H}_5)(\text{binap})]^+$  (**2**), based on DFT calculations performed on their models. The calculated coordination geometry reproduced the experimental parameters. Calculations on related models that do not exhibit this interaction, led to higher-energy species, and gave an estimate of the Mo– $\eta^2$ -arene interaction as 13.4 kcal mol<sup>-1</sup>, while the Ru– $\eta^2$ -arene interaction was 21.4 kcal mol<sup>-1</sup>. Energy decomposition analysis indicates that the favorable interaction is due to the coordination of the C=C bond, while much energy was needed to reorganize the ligand that must adapt to the new coordination environment.

*This work has been undertaken as a part of a European collaborative COST project (D24/0014/02). P. J. Costa acknowledges Fundação para a Ciência e Tecnologia (FCT) for a grant (SFRH/BD/10535/2002). M. J. Calhorda and P. J. Costa thank FCT for financial support (project POCI/QUI/58925/2004).*

## REFERENCES

1. Knobler C. B., Marder T. B., Mizusawa E. A., Teller R. G., Long J. A., Behnken P. E., Hawthorne M. F.: *J. Am. Chem. Soc.* **1984**, *106*, 2990.
2. Cheng T.-Y., Szalda D. J., Bullock R. M.: *Chem. Commun.* **1999**, 1629.
3. Tagge C. D., Bergman R. G.: *J. Am. Chem. Soc.* **1996**, *118*, 6908.
4. a) Mezetti A., Tschumper A., Consiglio G.: *J. Chem. Soc., Dalton Trans.* **1995**, 49; b) Bolm C., Kaufmann D., Gessler S., Harms K.: *J. Organomet. Chem.* **1995**, *502*, 47.
5. Pathak D. D., Adams H., Bailey N. A., King P. J., White C.: *J. Organomet. Chem.* **1994**, *479*, 237.
6. Feiken N., Pregosin P. S., Trabesinger G.: *Organometallics* **1997**, *16*, 5756.
7. a) Cyr P. W., Rettig S. J., Patrick O. B., James B. R.: *Organometallics* **2002**, *21*, 4672; b) Aneetha H., Jiménez-Tenorio M., Puerta M. C., Valerga P., Mereiter K.: *Organometallics* **2002**, *21*, 628.
8. a) Yin J., Rainka M. P., Zhang X.-X., Buchwald S. L.: *J. Am. Chem. Soc.* **2002**, *124*, 1162; b) Geldbach T. J., Pregosin P. S., Rizzato S., Albinati A.: *Inorg. Chim. Acta* **2006**, *359*, 962.
9. a) Deacon G. B., Forsyth C. M., Junk P. C., Skelton B. W., White A. H.: *Chem. Eur. J.* **1999**, *5*, 1452; b) Deacon G. B., Feng T., Skelton B. W., White A. H.: *Aust. J. Chem.* **1995**, *48*, 741; c) Deacon G. B., Nickel S., MacKinnon P., Tiekink: *Aust. J. Chem.* **1990**, *43*, 1245.
10. a) Hayashi T. J.: *Acc. Chem. Res.* **2000**, *33*, 354; b) Geldbach T. J., Pregosin P. S.: *Eur. J. Inorg. Chem.* **2002**, 1907.
11. Hölscher M., Franciò G., Leitner W.: *Organometallics* **2004**, *23*, 5606.
12. Novak A., Fryatt R., Woodward S.: *C. R. Chim.* **2007**, in press; doi:10.1016/j.crci.2006.10.008.
13. Li Q.-S., Wan C.-Q., Zou R.-Y., Xu F.-B., Song H.-B., Wan X.-J., Zhang Z.-Z.: *Inorg. Chem.* **2006**, *45*, 1888.
14. Muir K. W., Ibers J. A.: *Inorg. Chem.* **1970**, *9*, 440.
15. Green M. L. H., Brookhart M.: *J. Organomet. Chem.* **1983**, *250*, 395.

16. Parr R. G., Yang W.: *Density Functional Theory of Atoms and Molecules*. Oxford University Press, New York 1989.
17. a) *ADF2004.01*, SCM, Theoretical Chemistry, Vrije Universiteit, Amsterdam, The Netherlands; <http://www.scm.com>; b) te Velde G., Bickelhaupt F. M., van Gisbergen S. J. A., Guerra C. F., Baerends E. J., Snijders J. G., Ziegler T.: *J. Comput. Chem.* **2001**, *22*, 931; c) Guerra C. F., Snijders J. G., te Velde G., Baerends E. J.: *Theor. Chem. Acc.* **1998**, *99*, 391.
18. Vosko S. H., Wilk L., Nusair M.: *Can. J. Phys.* **1980**, *58*, 1200.
19. a) Versluis L., Ziegler T.: *J. Chem. Phys.* **1988**, *88*, 322; b) Fan L., Ziegler T.: *J. Chem. Phys.* **1991**, *95*, 7401.
20. Perdew J. P., Chevary J. A., Vosko S. H., Jackson K. A., Pederson M. R., Singh D. J., Fiolhais C.: *Phys. Rev. B* **1992**, *46*, 6671.
21. van Lenthe E., Ehlers A., Baerends E. J.: *J. Chem. Phys.* **1999**, *110*, 8943.
22. a) Mayer I.: *Chem. Phys. Lett.* **1983**, *97*, 270; b) Mayer I.: *Int. J. Quantum Chem.* **1984**, *26*, 151.
23. Wiberg K. B.: *Tetrahedron* **1968**, *24*, 1083.
24. a) Carpenter J. E.: *Ph.D. Thesis*. University of Wisconsin, Madison (WI) 1987; b) Carpenter J. E., Weinhold F.: *J. Mol. Struct.* **1988**, *169*, 41; c) Foster J. P., Weinhold F.: *J. Am. Chem. Soc.* **1980**, *102*, 7211; d) Reed A. E., Weinhold F.: *J. Chem. Phys.* **1983**, *78*, 4066; e) Reed A. E., Weinhold F.: *J. Chem. Phys.* **1985**, *83*, 1736; f) Reed A. E., Weinstock R. B., Weinhold F.: *J. Chem. Phys.* **1985**, *83*, 735; g) Reed A. E., Curtiss L. A., Weinhold F.: *Chem. Rev.* **1988**, *88*, 899; h) Weinhold F., Carpenter J. E.: *The Structure of Small Molecules and Ions*. Plenum Press, New York 1988.
25. Glendening E. D., Badenhoop J. K., Reed A. E., Carpenter J. E., Bohmann J. A., Morales C. M., Weinhold F.: *NBO 5.0*. Theoretical Chemistry Institute, University of Wisconsin, Madison (WI) 2001.
26. a) Ziegler T., Rauk A.: *Theor. Chim. Acta* **1977**, *46*, 1; b) Ziegler T., Rauk A.: *Inorg. Chem.* **1979**, *18*, 1558; c) Ziegler T., Rauk A.: *Inorg. Chem.* **1979**, *18*, 1755.